Comparison of random and periodic rough surfaces by ultrasonic attenuation and frequency distribution

Hiroyuki Nakamoto, Kazuma Terada, Philippe Guy, Tetsuya Uchimoto

Comparison of random and periodic rough surfaces by ultrasonic attenuation and frequency distribution

Hiroyuki NAKAMOTO*,[1], Kazuma TERADA[1], Philippe GUY[2], Tetsuya UCHIMOTO[3,4]

[1] *Graduate School of System Informatics, Kobe University, 1-1 Rokkodai, Nada, Kobe 657-8501, Japan*

[2] *Laboratoire Vibrations Acoustique, INSA-Lyon, 25 bis, av. J. Capelle 69621 Villeurbanne Cédex, France*

[3] *Institute of Fluid Science, Tohoku University, 2-1-1 Katahira, Aoba-ku, Sendai, 980-8577, Japan*

[4] *ELyTMaX IRL3757, CNRS, Univ Lyon, INSA Lyon, Centrale Lyon,*

Université Claude Bernard Lyon 1, Tohoku University,

2-1-1 Katahira, Aoba-ku, Sendai, Japan

***** *Correponding author : Graduate School of System Informatics, Kobe University, 1-1 Rokkodai, Nada, Kobe 657-8501, Japan, Tel:+81-78-8036669, E-mail:nakamoto@panda.kobe-u.ac.jp*

Abstract. Flow accelerated corrosion generates not only pipe-wall thinning but also roughness on an inside wall. In some flow conditions, the increase in roughness can increase the mass transfer coefficient by up to 80%. It is then very important to have an evaluation tool to monitor and quantify the roughness of a pipe. This study aims to estimate the roughness by using ultrasonic attenuation. The advantage of using ultrasonic attenuation is that it utilizes the signals measured by existing ultrasonic probes, and does not require significant changes to the equipment. To evaluate the inner rough surface, this study compares ultrasonic attenuations on random and periodic rough surfaces. We used an ultrasonic broadband probe on specimens with random and periodic rough surfaces in experiments. The results indicate a significant difference between the attenuation values estimated on random and periodic roughness. In addition, attenuation of amplitude at specific frequencies also was observed. These specific frequencies implied having the potential to estimate the pitch of periodic flaws on the rough surface.

Keywords: nondestructive testing, ultrasonic attenuation, rough surface

1 Introduction

In nuclear power plants, the cooling piping system is one of the essential components. Electric power supply companies need to maintain the health of pipes to keep a stable flow in them. The flows generate corrosion and erosion on the inside wall of the pipe. The corrosion and erosion wear the inside wall and decrease the thickness of the pipe wall. Hence, in general, inspectors measure the thickness of the pipe wall to assess the health of the pipe. However, the corrosion and erosion phenomena not only act on the thinning of the pipe wall but also in getting the inner surface of the pipe wall rougher. Pietralik reported the inner surface becomes rough as a result of flow accelerated corrosion (FAC) degradation [1]. Poulson showed scalloped surfaces on the inside pipe wall [2]. These rough surfaces reduce the mechanical strength of the pipe and finally induce bursting in the case of high-pressure flow. Also, they promote mass transfer and accelerate the pipe-wall thinning [3]. Therefore, the inspectors need to measure both the thickness and roughness of the pipe.

Various methods are used to measure roughness. Ghodrati et al. proposed an image processing method to measure randomly rough metallic surfaces [4]. Quan and Yuan reported that an optical fiber sensor measured roughness with a precision of 10 nanoscales [5]. Vértesy et al. confirmed the potential for roughness measurement by magnetic adaptive testing and Barkhausen noise measurement [6]. Although such optical and electromagnetic methods are sensitive to surface roughness, measurement of the roughness on an inner surface of a pipe with nondestructive is difficult. Studies for roughness measurement have dealt with ultrasonic scattering on a rough surface by the Kirchhoff approximation [7, 8]. Pettit et al. calculated both the coherent signal and the total scattered field using a finite element model and compared them with Kirchhoff theory predictions [9]. Shi et al. calculated the scattered field of an ultrasonic wave with Monte Carlo simulation and also proposed a correlation function to reconstruct rough surfaces [10, 11]. Their studies focused on the enhancement of theoretical equations. Nguyen et al. reported an estimation method of the pitch of rough surfaces using ultrasonic waves from different angles. Although their

experimental data showed high accuracy in pitch measurement, the rough surface has both random and periodic characteristics [12].

To estimate the roughness of the piping inner surface, Nakamoto [13] has reported that, in accordance with Nagy's model [14], the reflection on an ultrasonic beam at normal incidence on a rough surface leads to attenuation due to the scattering of the wavefront. In a previous paper [13], we described the results obtained on simulated periodic roughnesses. The advantage of using ultrasonic attenuation is that it utilizes the signals measured by existing ultrasonic probes, and does not require significant changes to the measurement device. In the present study, we compare these latter to those obtained on the other specimen exhibiting random roughnesses. Experimental results show a significant difference between both kinds of specimens. Also, we verify that the rough surface with a periodic flaw attenuates the spectrum of the specific frequency of the ultrasonic wave.

2 Method

2.1 Attenuation on rough surface

In this study, we consider a beam of longitudinal ultrasonic waves generated by a commercial piezoelectric probe. As shown in Fig. 1, the wave travels from the outer surface of the pipe, through the thickness of the tested specimen and is scattered by the inner rough surface. The reflected and attenuated wave is received by the same probe used in pulse-echo mode. The relationship between the reflection coefficient r of the ultrasonic wave on the rough surface and the roughness h of the surface is as follows:

$$r = r_0 e^{-2k^2h^2}, \tag{1}$$

where k is wave number, h is the root-mean-squared height of the rough surface [14], and r_0 is the reflection coefficient on a flat surface of the same material. Eq. (1) indicates that the wave number and the roughness attenuate ultrasonic waves. Because the wavelength determines the wave number, the roughness is the essential factor affecting the attenuation.

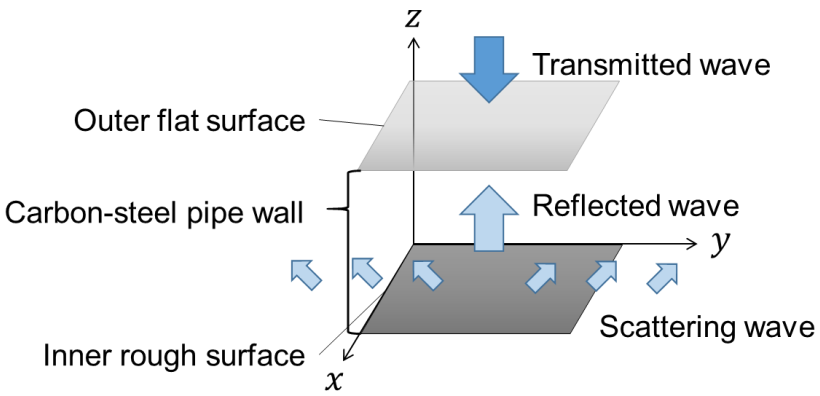

Fig. 1 Transmitted wave on outer flat surface and reflected wave on inner rough surface.

In experiment, we consider the ratio of the amplitude of the second reflected wave to that of the first reflected wave, because the reflected waves are attenuated by not only the rough surface but also other intrinsic factors in steel or in the couplant. So, to cancel the other factors except for the inner rough surface, we use the first and second reflected waves. Fig. 2 shows the schematic of measurement of the first and second reflected waves. $A0, A^{1st}$, and A^{2nd} are the amplitudes of the transmitted, first reflected, and second reflected waves, respectively. The ratio of the amplitude of the first reflected wave to that of the second reflected wave corresponds to the reflection coefficient r. Hence, when the amplitudes of the first and second reflected waves on the flat surface are A_0^{1st} and A_0^{2nd}, respectively, the following equation is derived [13].

$$\frac{\frac{A^{2nd}}{A^{1st}}}{\frac{A_0^{2nd}}{A_0^{1st}}} \approx \frac{r}{r_0} = e^{-k^2h^2}. \tag{2}$$

Using Eq. (2), we can compare the experimental and theoretical data. In this expression, the exponential term represents the attenuation factor due to the sole roughness effect. The attenuation factor due to the propagation and the scattering and/or viscosity is canceled because of the normalization by the reference waves.

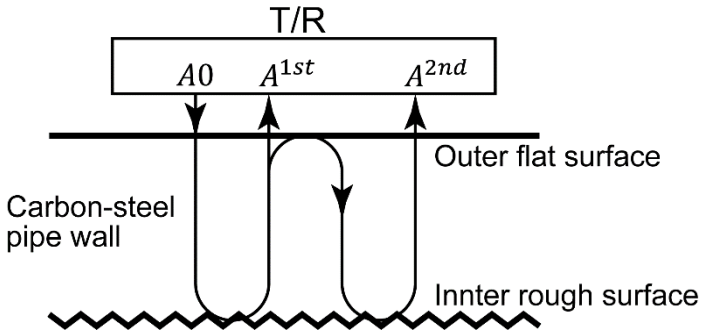

Fig. 2 Measurement of the amplitudes of the first and second reflected waves on the inner rough surface.

2.2 Frequency analysis

The theoretical model assumes that a generated ultrasonic wave is harmonic and hence has a single well-defined frequency. Actually, a piezoelectric probe generates waves with a large frequency bandwidth. So the frequency spectrum of the incident and reflected waves are not Dirac functions but a Gaussian-like distribution. In the following, we will study the frequency spectra of reflected waves from surfaces of varying roughness to confirm not only ultrasonic attenuation but also the frequency with much-attenuated amplitude.

3 Experiments

3.1 Experimental Instrument

The main element of the experimental setup is an ultrasonic probe of 8 mm in diameter, with a central frequency of 5 MHz and as can be seen in Fig. 4 (a), its bandwidth is about 3 MHz. The transducer is driven by a pulser that delivers a short pulse. The constitutive devices of the

setup are listed in Table 1. Then the receiver amplified the received signal by a factor of 1.5. The data acquisition system digitized and recorded the amplified signal by the sampling frequency of 2 GHz.

Table 1 Devices of experimental instrument.

Pulser and receiver	JPR-600C, Japan Probe Co, Japan
Broadband longitudinal probe	B5C5N, Japan Probe Co, Japan
Data acquisition	MSO-X 2014A, Agilent Technologies, Inc. USA

3.2 Comparison of random and periodic rough surfaces

Specimens were three carbon steel blocks of 20 mm in thickness and an area of 40×40 mm^2 as shown in Fig. 3. They exhibit simulated rough surfaces. One has a randomly rough surface made by blast machining on one side surface. The roughness calculated from the height profile was 25.0 μm. The others had periodic and rectangular flaws obtained by machining on one side surface. The physical characteristics of the specimens are presented in Table 2. The opposite sides of their rough surfaces were flat. The roughnesses of P125 and P200 are design values.

A probe and a pulser-receiver instrument transmitted and received ultrasonic waves from the flat side of the specimens. We performed 10 measurements for each specimen of the first and second reflected waves. In addition, a specimen without flaws was used to obtain the amplitudes A_0^{1st} and A_0^{2nd} of the reflection wave on a flat surface, which is used for calculation in Eq. (2).

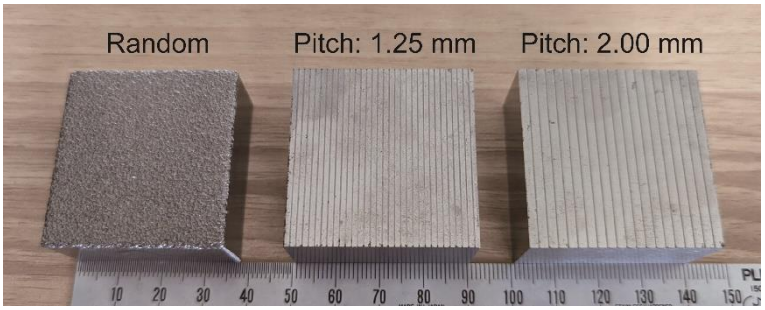

Fig. 3 One random and two periodic flaw specimens.

Table 2 Physical characteristics of specimens

Specimen	Type	Roughness [μm]	Depth [μm]	Width [μm]	Pitch [mm]
Random	Random	25.0	144(P-P)	-	-
P125	Periodic	39.1	100	250	1.25
P200	Periodic	32.4	100	250	2.00

Figure 4 shows the evolution of the theoretical and experimental attenuations with frequency and typical spectra of the first and second reflection waves. The attenuation values of the random specimen fit quite well with the theoretical model in the frequency range between 2.5 and 5 MHz. Outside of this bandwidth, the reflected spectrum on the rough specimen is not exploitable because of the decrease of the second spectrum at high frequency. The attenuation value of P125 specimen fitted to the theoretical line in the narrow range from 3 to 4 MHz in comparison with the random specimen. Also, P200 specimen fitted to the theoretical line in the narrow range from 3.5 to 5 MHz. Even though the specimens had approximately the same roughness, the random specimen fitted the theoretical line better. The periodic characteristics of the rough surface might make the difference between the random and the others. P125 specimen had the spectrum distribution of the first reflection wave with the complex shape which had a small drop at 5 MHz in Fig. 4 (b). At the frequency of this drop, the attenuation value was separated from the theoretical line. P200's attenuation value also was separated at 3 MHz which made the high standard deviation values in comparison with the random specimen. So, the experimental data revealed the difference between the random and periodic roughness.

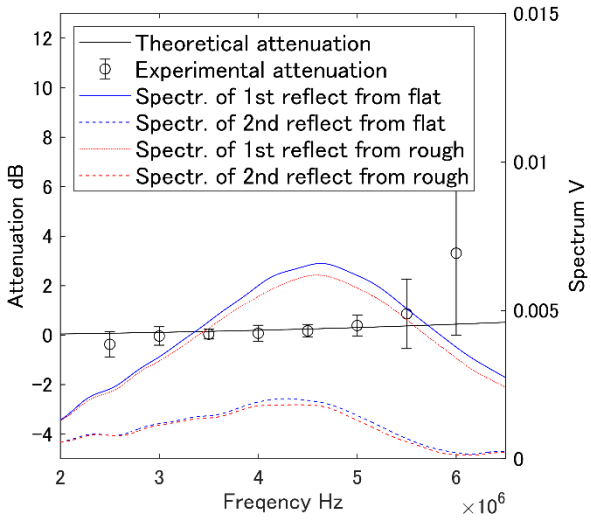

(a) Random

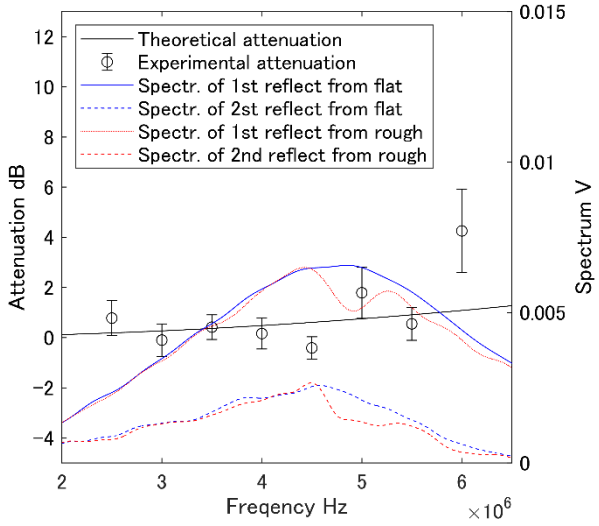

(b) P125

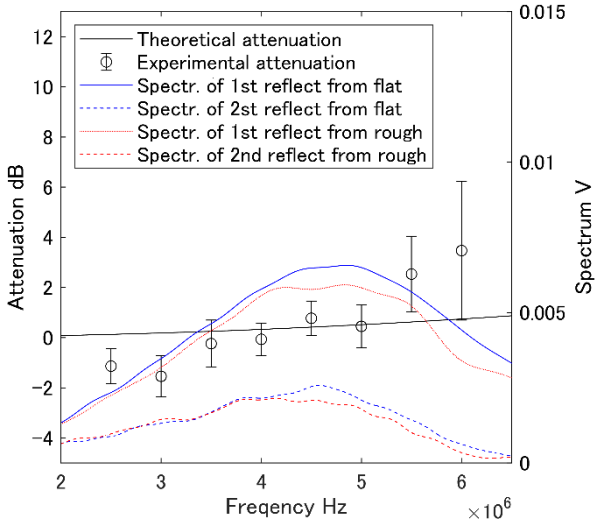

(c) P200

Fig. 4 Relationship between frequency and attenuation value and the example spectra.

3.3 Effect of roughness and flaw pitch on spectrum

To confirm the effect of roughness and flaw pitch on the spectrum, specimens with different flaw depths were added to P125 and P200 specimens. They are 20 mm in thickness with an area of 40×40 mm^2. The characteristics of the specimens including P125 and P200 are listed in Table 3. The flaw width of all specimens is constant and 250 μm. The roughnesses of the specimen, which are design values, are in the range of approximately 20 and 70 μm.

Table 3 Physical characteristics of specimens with different flaw depth.

Specimen	Roughness [μm]	Depth [μm]	Pitch [mm]
P125-20	20.0	50	1.25
P125-35	39.1	100	1.25
P125-55	56.0	140	1.25
P125-70	72.0	180	1.25
P200-20	19.8	60	2.00
P200-35	33.1	100	2.00
P200-55	56.2	170	2.00
P200-70	72.8	220	2.00

The broadband probe of 5 MHz generated a normal beam and received the first reflection in pulse-echo mode. The number of measurements was 10. The means of the spectra are shown in Fig. 5. The rougher surface attenuated the ultrasonic wave more around 5 MHz. The spectra exhibit drops at specific frequencies. For the P125 sample, the principal deep is observed at 4.9 MHz, which corresponds to a wavelength of 1.21 mm very close to the flaw pitch of 1.25 mm. Also, for the P200 sample, a drop is observed at 3.0 MHz, which corresponds to a wavelength of 1.97 mm again very close to the flaw pitch of 2.00 mm. Since these drops are only observed for the periodic roughnesses, we assume that this could be due to diffraction phenomena, but this is to be investigated in the future.

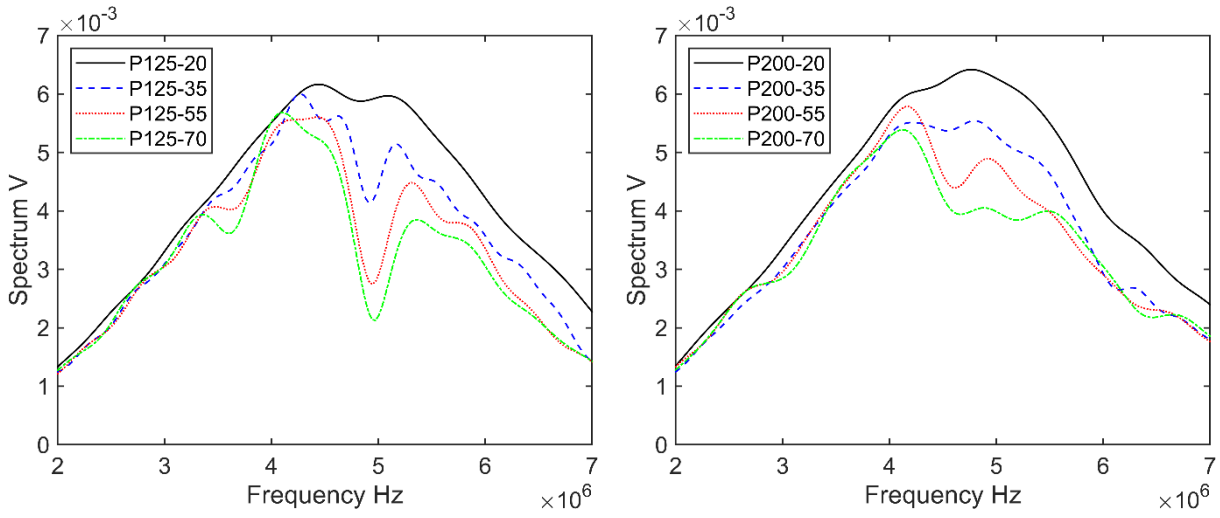

(a) Pitch: 1.25 mm.

(b) Pitch: 2.00 mm.

Fig. 5 Spectra of the first reflection wave on the different rough surfaces.

4 Conclusion

We compared the random roughness with the simulated periodic roughness in this study. The attenuation value of the random roughness fitted well with the theoretical value. Those of the periodic roughness were not so. We confirmed a significant difference between both kinds of specimens. We also verified that the rough surface with a periodic flaw attenuates the spectrum of the specific frequency of the ultrasonic wave. The wavelength calculated from the attenuated frequency corresponded to approximately the flaw pitch of the rough surface. This indicates the potential of the estimation of flaw pitch from the reflected broadband wave. In future work, we make a variety of flaw pitches and verify the difference in the spectrum distribution. A specimen with both random and periodic roughness should be tested. After that, we will propose a frequency selection method to estimate roughness.

Acknowledgements

Part of the work was carried out under the Collaborative Research Project of the Institute of Fluid Science, Tohoku University.

References

[1] J.M. Pietralik, The Role of Flow in Flow-Accelerated Corrosion under Nuclear Power Plant Conditions, *E-J. Adv. Maintenance*, **4**, (2012) 63-78.

[2] B. Poulson, Predicting and Preventing Flow Accelerated Corrosion in Nuclear Power Plant, *Int. J. Nuclear Energy*, **2014** (2014), Article ID 423295. doi:10.1155/2014/423295

[3] N. Fujisawa, K. Uchiyama and T. Yamagata, Mass transfer measurements on periodic roughness in a circular pipe and downstream of orifice, *Int. J. Heat and Mass Transfer*, **105** (2017), 316-325. doi:10.1016/j.ijheatmasstransfer.2016.10.002

[4] S. Ghodrati, S. G. Kandi and M. Mohseni, Nondestructive, fast, and cost-effective image processing method for roughness measurement of randomly rough metallic surfaces, J. Opt. Soc. Am. A, 35 (2018), 998-1013. doi:10.1364/JOSAA.35.000998

[5] Z. Quan and L. Yuan, High precision roughness sensor based on annular core optical fiber, Rev. Sci. Instrum., 91 (2020), 065001. doi:10.1063/5.0001603

[6] G. Vértesy, A. Gasparics, J.M. Griffin, J. Mathew, M.E. Fitzpatrick, I. Uytdenhouwen, Analysis of Surface Roughness Influence in Non-Destructive Magnetic Measurements Applied to Reactor Pressure Vessel Steels, Appl. Sci., 10 (2020), 8938. doi:10.3390/app10248938

[7] J.A. Ogilvy, Theoretical comparison of ultrasonic signal amplitudes from smooth and rough defects, *NDT International*, **19** (1986), 371-385. doi:10.1016/0308-9126(86)90028-3

[8] E.I. Thorsos, The validity of the Kirchhoff approximation for rough surface scattering using a Gaussian roughness spectrum, *J. the Acoust. Soc. of Am.* **83** (1988), 78-92. doi:10.1121/1.396188

[9] J.R. Pettit, A.E. Walker and M.J.S. Lowe, Improved detection of rough defects for ultrasonic nondestructive evaluation inspections based on finite element modeling of

elastic wave scattering, *IEEE Trans. on Ultrason. Ferroelectr. Freq. Control*, **62** (2015), 1797-1808. doi:10.1109/TUFFC.2015.007140

[10] F. Shi, M.J.S. Lowe, X. Xi and R.V. Craster, Diffuse scattered field of elastic waves from randomly rough surfaces using an analytical Kirchhoff theory, *J. the Mecha. and Phys. of Solids*, **92** (2016), 260-277. doi:10.1016/j.jmps.2016.04.003

[11] F. Shi, M.J.S. Lowe and R.V. Craster, Recovery of correlation function of internal random rough surfaces from diffusely scattered elastic waves, *J. the Mech. and Phys. of Solids*, **99** (2017), 483-494. doi:10.1016/j.jmps.2016.11.003

[12] C.N. Nguyen, M. Sugino, Y. Kurokawa and H. Inoue, Ultrasonic evaluation of the pitch of periodically rough surfaces from back side, *Mech. Eng. J.*, **4** (2017), 17-00278. doi:10.1299/mej.17-00278

[13] H. Nakamoto, P. Guy and T. Takagi, Corrosion Induced Roughness Characterization by Ultrasonic Attenuation Measurement, *E-J. of Adv. Maintenance*, **11** (2020), 139-146.

[14] P.B. Nagy and L. Adler, Surface roughness induced attenuation of reflected and transmitted ultrasonic waves, *J. the Acoust. Soc. of Am.*, **82** (1987), 193-197. doi:10.1121/1.395545